論文 / 著書情報
Article / Book Information

論題(和文)	
Title	SrTiO3-based sensors for in situ monitoring of trace levels of oxygen
著者(和文)	原亨, 石黒隆
Authors	Toru Hara, Takashi Ishiguro
出典 / Citation	J. Ceram. Soc. Jpn., Vol. 118, , p. 300
Citation(English)	J. Ceram. Soc. Jpn., Vol. 118, , p. 300
発行日 / Pub. date	2010, 4

Journal of the Ceramic Society of Japan 118 [4] 300-304 2010 Paper

$SrTiO_3$-based sensors for in situ monitoring of trace levels of oxygen

Toru HARA† and Takashi ISHIGURO

Corporate Technology Planning Department, Research and Development Laboratory, Taiyo Yuden Co., Ltd., 8–1 Sakae-cho, Takasaki, Gunma 370–8522

Semiconductive dielectric $SrTiO_3$ thin films are promising candidates for the in situ monitoring of trace levels of oxygen in semiconductor manufacturing processes. Highly sensitive oxygen sensors were prepared by atomic-layer deposition (ALD) or pulsed-laser deposition (PLD) of $SrTiO_3$; however, there was a problem with ALD-$SrTiO_3$ that surface defects, such as SrO surface segregation with a minor contribution from SrO_2, affected the detection below an oxygen concentration [$P_{O2}/(P_{O2} + P_{He})$] of 1.1×10^{-12}, causing the reversion of ALD-$SrTiO_3$ to a slightly high-resistance state. The coverage of the segregated surface of SrO and SrO_2 on the ALD-$SrTiO_3$ was considerably higher than that observed on the PLD-$SrTiO_3$ surface, however, the reversion could be markedly suppressed by the additional thermal treatment, probably owing to gathering small SrO-based surface islands (building-up of bigger islands), resulting in the exposure of clean surfaces.

Key-words : Oxygen sensor, $SrTiO_3$ thin film, Atomic-layer deposition, Pulsed-laser deposition

[Received December 7, 2009; Accepted January 15, 2010]

1. Introduction

Semiconductive dielectric $SrTiO_3$ thin films are promising candidates for the in situ monitoring of trace levels of oxygen (e.g., 1–10 ppb) in semiconductor manufacturing processes. In our previous studies, it was found that $SrTiO_3$ thin films prepared using atomic-layer deposition (ALD)[1] or pulsed-laser deposition (PLD)[2),3] detect oxygen contamination on the ppb order. Although PLD is ideal for basic research, it is not feasible for mass production since the use of plumes prevents the deposition of materials on the entire surface of the wafers on which devices are formed. ALD is a candidate process for mass production;[4)–7] however, there is a problem that the SrO surface segregation with a minor contribution from SrO_2, which can be a p-type semiconductor, affect the detection below an oxygen concentration [$P_{O2}/(P_{O2} + P_{He})$] of 1.1×10^{-12}, through the generation of p–n junctions between p-type SrO_{1+x} and n-type $SrTiO_3$.[1]

In this study, (1) the differences in the surface chemical composition of ALD-$SrTiO_3$ and PLD-$SrTiO_3$-based films and (2) the influences of the surface chemical composition on oxygen sensitivity were studied.

2. Experimental methods

2.1 Sample preparation

2.1.1 ALD of $SrTiO_3$ thin films

(110)-oriented 20-nm-thick $SrTiO_3$ films were deposited by ALD at 300°C onto 4-inch c-sapphire substrates with a thickness of 0.5 mm. During the ALD of $SrTiO_3$, $Sr(thd)_2$ (thd = 2,2,6,6-tetramethyl-3,5-heptanedionate) as the source material of strontium and $Ti(O\text{-}i\text{-}Pr)_4$ (O-i-Pr = isopropoxide) as the source material of titanium were alternately introduced into the ALD reactor (TFS 500, Beneq Oy) using nitrogen as the carrier and purging gas. Ozone and water vapor were used as oxygen sources after the introduction of $Sr(thd)_2$ and $Ti(O\text{-}i\text{-}Pr)_4$, respectively. The films were annealed at 700°C for 30 min in N_2 to crystallize the deposited amorphous films. Some specimens were thermally treated at 600°C for 30 min in air after the annealing in N_2. Ti/Au (20 nm thick/200 nm thick) layers were deposited by dc sputtering and electrodes were patterned by the lift-off technique (electrode gap of 6 μm, overlapping electrode length of 500 μm).

2.1.2 PLD of $SrTiO_3$-based thin films

In order to deposit (110)-oriented 50-nm-thick layer of $SrTiO_3$ or $SrTi_{0.9952}Cr_{0.0048}O_3$ (Cr:$SrTiO_3$ hereafter) by PLD, 20-nm-thick CeO_2-coated 8 at.% Y^{3+}-doped ZrO_2 (YSZ hereafter) (001) substrates were used. A KrF excimer laser ($\lambda = 248$ nm, energy = 190 mJ, repetition rate = 7 Hz) was irradiated onto targets. Sintered pellets of $SrTiO_3$ and CeO_2, and a single crystal of Cr:$SrTiO_3$ were used as targets. Oxygen was used as the reactive gas inside the chamber during the deposition, and the pressure was maintained at 7.3×10^{-2} Pa during the deposition and cooling to room temperature. During the deposition, substrates were heated up to 800°C. Pt electrodes (200-nm-thick, electrode gap of 250 μm, overlapping electrode length of 10 mm) were deposited by DC sputtering at 250°C onto the top surface of the specimens through metal masks.

$SrTiO_3$(110) substrates, which were annealed at 1,000°C in O_2 in order to decrease surface roughness, were also used; however, the deposited films were highly insulative probably owing to the surface roughness of the annealed $SrTiO_3$(110) substrates. The surface roughness of the $SrTiO_3$(110) substrates results from $SrO(H_2O)_n$ [$Sr(OH)_2$] or $SrCO_3$ surface segregation. The surface segregation cannot be completely removed since (110)-oriented $SrTiO_3$ cannot be treated by buffered aqueous solution of hydrofluoric acid, which is usually used for removing the surface segregation from $SrTiO_3$(001).[10] Therefore, the results on PLD films deposited onto CeO_2/YSZ(001) are compared with the results on (110)-oriented ALD films in this study.

PLD films with a thickness of 50 nm could be epitaxially grown onto CeO_2/YSZ substrates and could be sensitive to oxygen. PLD films with a thickness of 25 nm were also prepared;

† Corresponding author: T. Hara; t-hara@jtyyuden.co.jp

however, they could not be epitaxially grown (they were multiotiented. X-ray diffraction data not shown here.) and could not be sensitive to oxygen. Therefore, the results on 50-nm-thick PLD films are compared with the results on 20-nm-thick ALD films in this study. The in-plane lattice parameters of CeO_2 and YSZ(001) are 0.5419 and 0.5125 nm, respectively. These values are incompletely-matched with $\sqrt{2} \times 0.3905$ nm $= 0.552$ nm of $SrTiO_3$(110), where 0.3905 nm is the lattice parameter of cubic $SrTiO_3$ in bulk form. Such a mismatch may require the thickness of 50 nm in order to obtain well-oriented crystalline films.

2.2 Measurement of electrical resistance at various oxygen concentrations

The electrical resistances of the specimens were measured at room temperature using an Agilent 4349B high-resistance meter. An in-plane electric field of 1 V·μm^{-1} was applied between the electrodes. During the measurements, the specimens were placed in a test chamber. The concentration of oxygen, which was diluted in helium, was controlled by a gas calibration system.[1)] During the test, the total pressure was maintained at 10^5 Pa. Before the test, the specimens were heated to 130°C for 1 h in vacuum to eliminate molecules containing oxygen, which were adsorbed on the surfaces of the specimens.

2.3 Crystallite orientation analyses

In our previous study, the crystallite orientation of the 20-nm-thick ALD-$SrTiO_3$ film was investigated by transmission electron microscopy (TEM) and electron beam diffraction (EBD).[1)] The intensity of the peak in the θ–2θ X-ray diffraction (XRD) pattern of the ALD film was very low owing to the low thickness of the film (20 nm), which prevented us from conducting XRD analysis.

In this study, the crystallite orientations of the 50-nm-thick PLD-$SrTiO_3$-based films were characterized by XRD analyses using Cu Kα monochromatic radiation (0.154 nm) at 40 kV with a current of 30 mA (X'Pert-MPD, Philips).

2.4 Surface chemical analyses

To investigate the microstructure and chemical composition of the film surface, tapping mode atomic force microscopy (AFM), scanning electron microscopy (SEM), and angle-resolved X-ray photoelectron spectroscopy (ARXPS) were carried out using an SPA-400 (Seiko Instruments Inc.), an FE-SEM S-4700 (Hitachi, Ltd.), and a VG Theta Probe (Thermo Fisher Scientific Inc.) equipped with a monochromatized Al(Kα) X-ray source, respectively.

3. Results and discussion

Figure 1 shows the electrical resistances of ALD-$SrTiO_3$, PLD-$SrTiO_3$, and PLD-Cr:$SrTiO_3$ at various oxygen concentrations. ALD-$SrTiO_3$ exhibited lower resistance than those of PLD-$SrTiO_3$-based thin films. N_2 postannealing introduces conducting electrons into ALD-$SrTiO_3$, leading to its low resistance. It is assumed that valence band holes, which can contribute to maintain the oxygen sensitivity,[1)–3)] are generated owing to the depletion of Sr^{2+} in ALD-$SrTiO_3$ near the surface since the SrO surface segregation results in such depletion near the surface. During the postannealing at 700°C after ALD, SrO seeps slowly from the interior onto the surface.

The resistance of ALD-$SrTiO_3$ exhibited a reversion to a slightly high-resistance state below an oxygen concentration of 1.1×10^{-12}. In our previous study, it was suggested that surface defects, such as the SrO surface segregation with a minor

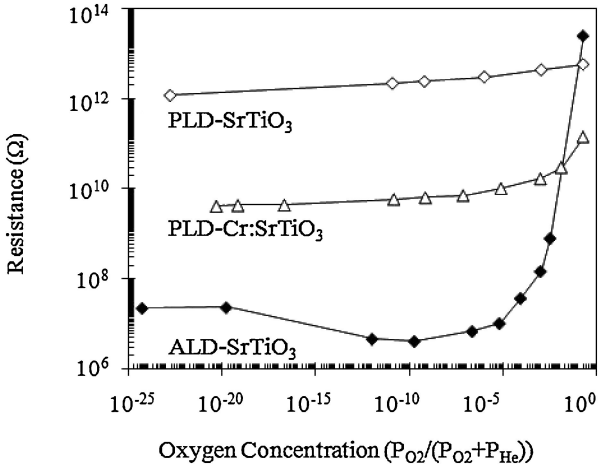

Fig. 1. Electrical resistances of ALD-$SrTiO_3$, PLD-$SrTiO_3$, and PLD-Cr:$SrTiO_3$ at various oxygen concentrations. The electrical resistance of ALD-$SrTiO_3$ was normalized using that at an overlapping electrode length of 10 mm, which is equal to the electrode length of the PLD specimens. It was not normalized for the electrode gap, since the applied electric field was 1 V·μm^{-1} for all the specimens.

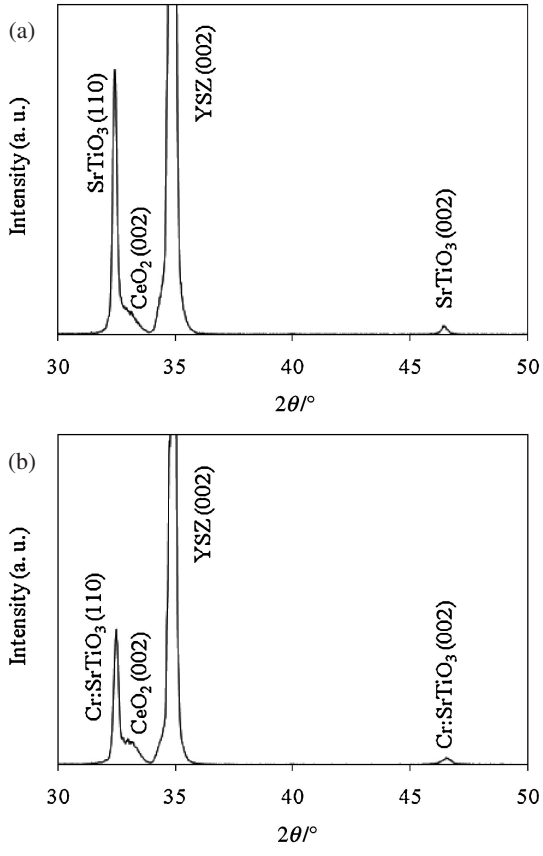

Fig. 2. θ–2θ X-ray diffraction (XRD) pattern of PLD-$SrTiO_3$/CeO_2/YSZ(001) substrate (a) and PLD-Cr:$SrTiO_3$/CeO_2/YSZ(001) substrate (b).

contribution from SrO_2 can affect the reversion to the slightly high-resistance state below an oxygen concentration of 1.1×10^{-12}, through the generation of p–n junctions.[1)]

The ALD-$SrTiO_3$ film is (110)-oriented with a minor contribution of (001) plane.[1)] The PLD-$SrTiO_3$ and PLD-Cr:$SrTiO_3$ films were mainly (110)-oriented, as shown in **Figs. 2**(a) and (b); the minor (100) plane could be observed, too.

Figures 3(a)–(d) shows SEM and AFM images of ALD-$SrTiO_3$ and PLD-Cr:$SrTiO_3$: SEM of ALD-$SrTiO_3$ (a), AFM of ALD-$SrTiO_3$ (b), SEM of PLD-Cr:$SrTiO_3$ (c), and AFM of PLD-Cr:$SrTiO_3$ (d). As shown in Figs. 3(a)–(d), the coverage of the segregated surface of ALD-$SrTiO_3$ was considerably higher than that observed on the PLD-Cr:$SrTiO_3$ surface. In general, SrO can easily seep from the interior onto the surface through grain boundaries during the postannealing in polycrystalline films, such as ALD-$SrTiO_3$, than in epitaxial films, such as PLD-Cr:$SrTiO_3$.

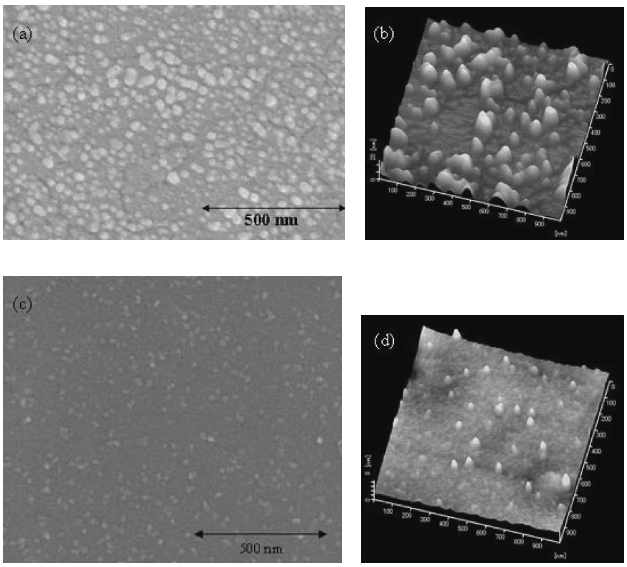

Fig. 3. Scanning electron microscopy (SEM) image and atomic force microscopy (AFM) image of ALD-$SrTiO_3$ and PLD-Cr:$SrTiO_3$: (a) SEM of ALD-$SrTiO_3$, (b) AFM of ALD-$SrTiO_3$, (c) SEM of PLD-Cr:$SrTiO_3$, and (d) AFM of PLD-Cr:$SrTiO_3$.

To investigate the surface chemical composition, ARXPS was carried out. **Figures 4**(a)–(d) show the Sr3d, Ti2p, O1s, and C1s core-level ARXPS spectra of ALD-$SrTiO_3$. As shown in Fig. 4(a), in addition to two peaks of $SrTiO_3$ (132.7 eV for $Sr3d_{5/2}$ and 134.4 eV for $Sr3d_{3/2}$), two peaks of the surface component, which mainly consists of SrO[8),9)] with a minor contribution from SrO_2,[9)] were observed at 133.8 eV ($Sr3d_{5/2}$) and 135.5 eV ($Sr3d_{3/2}$). The p-type SrO-based surface segregation and n-type $SrTiO_3$ can generate p–n junctions, causing the reversion to a slightly high-resistance state.[1)] As shown in Fig. 4(b), two emission lines of $SrTiO_3$ with a maximum at 458 eV ($Ti2p_{1/2}$) and 464 eV ($Ti2p_{3/2}$) were observed. As shown in Fig. 4(c), the peak of a surface contaminant (532 eV) was observed in addition to the O^{2-} ion peak of the metal oxide (529.2 eV). The surface contaminant is water and/or hydroxide adsorbed on the surface.[8)] As shown in Fig. 4(d), there was no peak around 290 eV indicating the presence of CO_3^{2-}-related species. **Figures 5**(a)–(d) show the ARXPS spectra of the PLD-Cr:$SrTiO_3$ film. As shown in Figs. 5(a)–(d), the surface segregation is markedly suppressed at the PLD-Cr:$SrTiO_3$ film surface. Probably owing to the sparse surface segregation, the PLD-Cr:$SrTiO_3$ film does not revert to the slightly high-resistance state below an oxygen concentration of 1.1×10^{-12}.

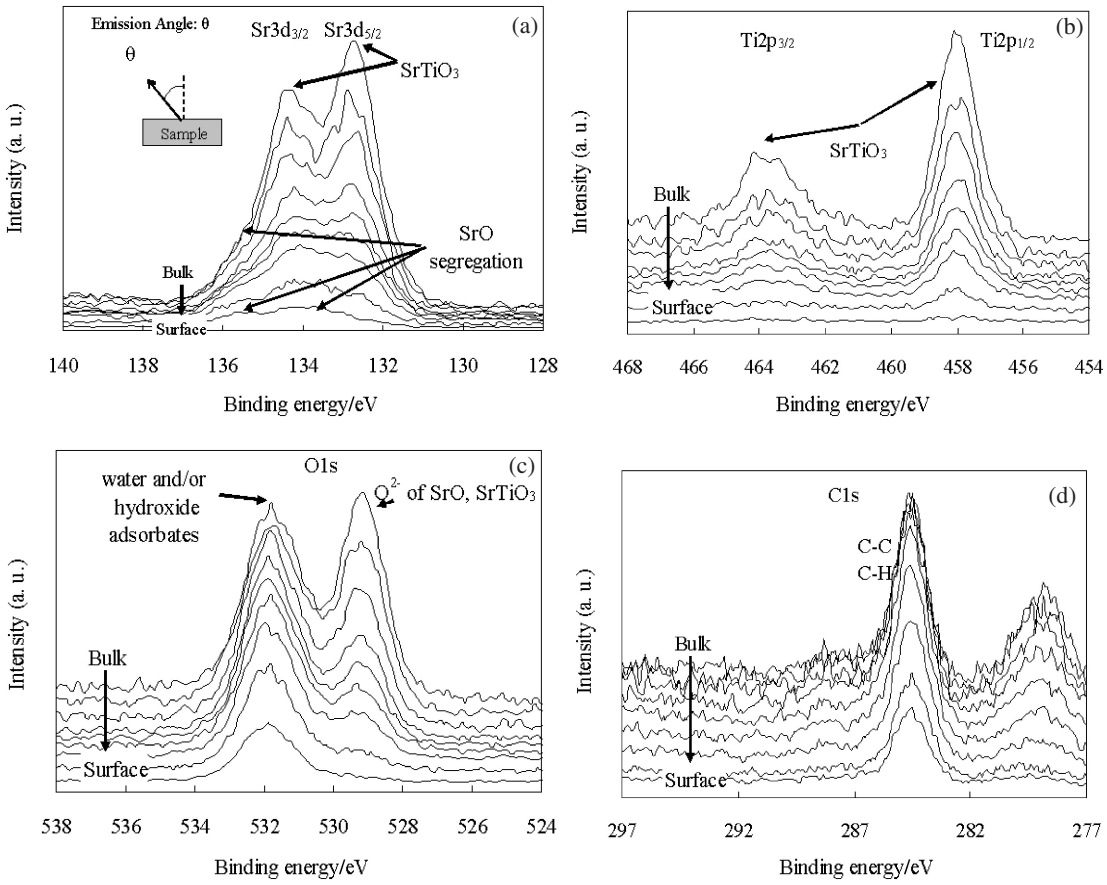

Fig. 4. Spectra obtained from angle-resolved X-ray photoelectron spectroscopy (ARXPS) of ALD-$SrTiO_3$: (a) Sr3d, (b) Ti2p, (c) O1s, and (d) C1s. The emission angle (θ) ranges from 24.875 degrees (emission from the bulk) to 81.125 degrees (emission from the surface).

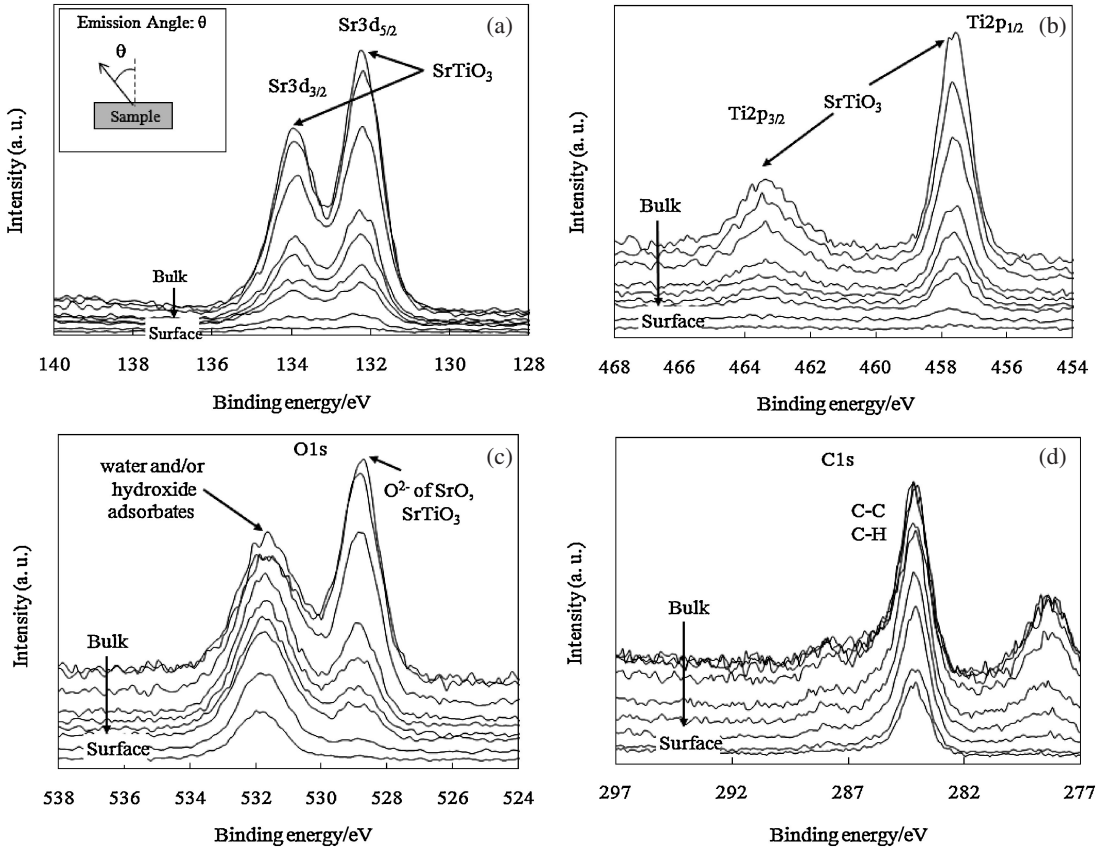

Fig. 5. Spectra obtained from angle-resolved X-ray photoelectron spectroscopy (ARXPS) of PLD-Cr:$SrTiO_3$ film: (a) Sr3d, (b) Ti2p, (c) O1s, and (d) C1s. The emission angle (θ) ranges from 24.875 degrees (emission from the bulk) to 81.125 degrees (emission from the surface).

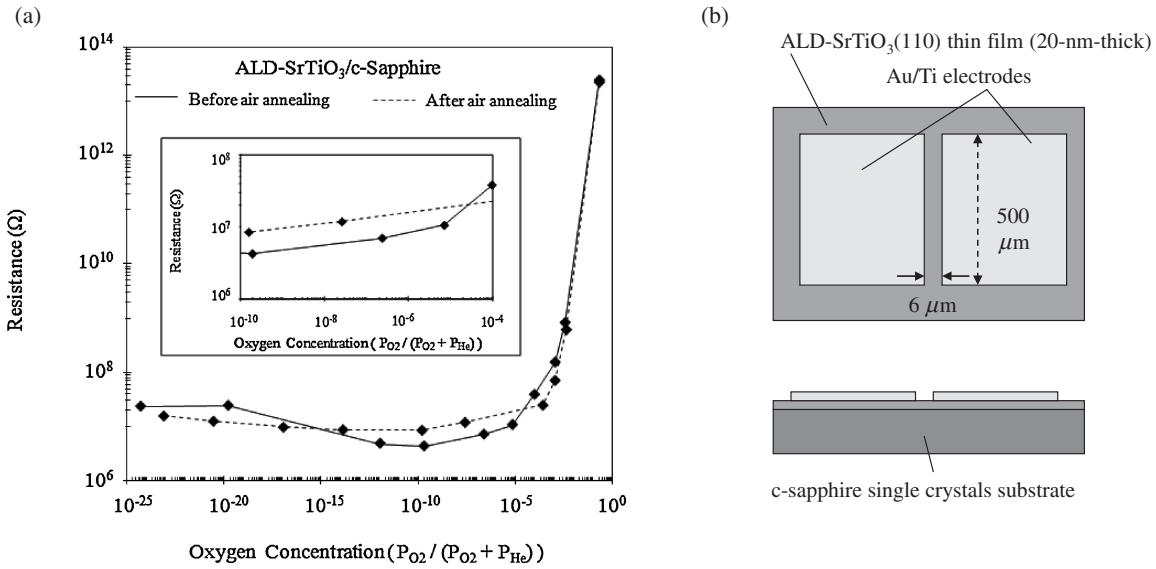

Fig. 6. (a) Electrical resistances of ALD-$SrTiO_3$ before and after an additional annealing in air at 600°C for 30 min. The electrical resistances were normalized using that at an overlapping electrode length of 10 mm. The inset displays the same data plot for the oxygen concentration range of 10^{-10}–10^{-4}. (b) Schematic picture of ALD-specimen.

Figure 6(a) shows the electrical resistances of ALD-$SrTiO_3$ before and after an additional annealing at 600°C in air. As shown in Fig. 6(a), the reversion to the high-resistance state was suppressed by the additional annealing. Sensitivity to oxygen concentrations of ppm–ppb order was maintained by the thermal treatment, although the resistance was slightly increased.

Figure 7 shows SEM images of ALD-$SrTiO_3$ surface before (left)/after (right) the additional annealing. As shown in Fig. 7, the additional annealing causes the small SrO-based surface islands to agglomerate, resulting in the exposure of clean $SrTiO_3$ surfaces. The additional annealing makes oxygen sensing at oxygen concentrations of 1.0×10^{-4}–1.0×10^{-9} more reliable.

Fig. 7. Scanning electron microscopic (SEM) images of ALD-$SrTiO_3$ surface before (left)/after (right) an additional annealing in air at 600°C for 30 min.

4. Conclusion

For ALD-$SrTiO_3$, the detection of oxygen below an oxygen concentration of 1.1×10^{-12} was affected by the reversion to a slightly high-resistance state. By investigating the differences in the surface chemical composition of ALD-$SrTiO_3$ film and PLD-$SrTiO_3$-based films, we concluded that the surface components (SrO and SrO_2) cause the reversion. The reversion to the high-resistance state was suppressed by an additional annealing, probably owing to gathering small SrO-based surface islands (building-up of bigger islands), resulting in the exposure of clean $SrTiO_3$ surfaces.

References

1) T. Hara and T. Ishiguro, *Sens. Actuators B Chem.*, 136, 489–493 (2009).
2) T. Hara, T. Ishiguro, N. Wakiya and K. Shinozaki, *Jpn. J. Appl. Phys.*, 47, 7486–7489 (2008).
3) T. Hara, T. Ishiguro, N. Wakiya and K. Shinozaki, *Mater. Sci. Eng. B*, 161, 142–145 (2009).
4) A. Kosola, M. Putkonen, L.-S. Johansson and L. Niinistö, *Appl. Surf. Sci.*, 211, 102–112 (2003).
5) H. Seim, H. Mölsä, M. Nieminen, H. Fjellvåg and L. Niinistö, *J. Mater. Chem.*, 7, 449–455 (1997).
6) M. Nieminen, S. Lehto and L. Niinistö, *J. Mater. Chem.*, 11, 3148–3153 (2001).
7) J. Päiväsaari, M. Putkonen and L. Niinistö, *J. Mater. Chem.*, 12, 1828–1832 (2002).
8) Q.-H. Wu, M. Liu and W. Jaegermann, *Mater. Lett.*, 59, 1980–1983 (2005).
9) B. Psiuk, J. Szade, H. Schroeder, H. Haselier, M. Mlynarczyk, R. Waser and K. Szot, *Appl. Phys., A Mater. Sci. Process.*, 89, 451–455 (2007).
10) T. Ohnishi, K. Shibuya, M. Lippmaa, D. Kobayashi, H. Kumigashira, M. Ohshima and H. Koinuma, *Appl. Phys. Lett.*, 85, 272–274 (2004).